Crystal Structures of *n*-Alkanes with Branches of Different Size in the Middle

Keisuke Ikedou,† Hiroko Yamamoto,* Hideo Nagashima, and Norio Nemoto

Department of Molecular and Material Sciences, IGSES, Kyushu University, 6−1 Kasuga-koen, Kasuga, Fukuoka 816-8580, Japan

Kohji Tashiro

Department of Future Industry-Oriented Basic Science and Materials, Toyota Technological Institute, 2−12−1 Hisakata, Tenpaku, Nagoya 468-8511, Japan

Received: December 26, 2004; In Final Form: April 11, 2005

We synthesized four branched *n*-alkane samples C35−C1, C35−C4, C35−C6, and C35−C4Ph with the same number of carbons as the main chain, $n = 35$, to which the methyl, butyl, hexyl, and butyl phenyl groups were respectively attached at the middle, and also the corresponding linear homologue of C35, and studied their crystalline structures from DSC, IR, and Raman spectroscopy, X-ray diffraction measurement, and computer simulation. Solid−solid phase transitions characteristic of linear alkane C35 are not observed for any branched alkanes, and their melting temperatures T_m are lowered to 325.2, 318.5, 314.3, and 314.1K, respectively. Main chains of branched alkane molecules are not folded, irrespective of length and chemical structure of branches, but are extended to take the planar zigzag form in the solid state. The branches of C35−C4 and C35−C6 are also aligned inside the crystal in the extended form. Data analyses on solution-grown crystallized samples reveal that, with increasing the branch length, their crystal structures transform from polymorphic forms of the orthorhombic ($P2_12_12_1$) and the triclinic ($P\bar{1}$) for C35−C1 and C35−C4 to the unique triclinic form for C35−C6 and C35−C4Ph, so as to minimize extra surface energy invoked by introduction of long branches.

Introduction

Linear *n*-alkanes with carbon numbers less than 80 are known to take the extended chain conformation as the energetically most favored form in the crystalline state, and the smooth flat interface is always formed between lamellae.[1−7] Introduction of small functional groups such as the carbonyl or hydroxyl group to the middle of those linear chains hardly disturbs the crystalline structure of their linear homologues.[8−17] The subcell structure is the same for all samples examined, and their melting temperatures become higher than those of the linear homologues because of dipole−dipole interaction or hydrogen bonding, whereas the solid−solid phase transitions characteristic of pure linear alkanes disappear due to this interaction.[3,18−22]

Among various branching effects on morphologies and crystalline structures of alkane molecules, the size effect can be most effectively studied introducing groups having only the van der Waals interaction to the main chain, and where the methyl group is the smallest unit. In a recent study on methyl-branched alkane, $(C_{19}H_{39})_2$ $CH(CH_3)$, denoted M39, we found that it crystallizes as an extended chain with the methyl group being inside the lamellae, and the crystals obtained with the solution-grown and bulk-crystallization methods both exhibit polymorphs taking two different crystalline structures belonging to the space groups $P\bar{1}$ and $P2_12_12_1$.[23] Compatibility tests between M39 and its linear homologue C39 indicated that, due to differences in their crystalline structures, the respective molecules, allowing a small amount of contamination of another component, tend to develop their own crystal structures separately over the entire range of molar fraction of M39 from 0.05 to 0.95 studied. The results are in contrast with a series of works reported by Ungar et al.,[24] who used symmetric as well as asymmetric longer branched alkane samples. They showed that either an extended or a once-folded chain conformation is realized depending on crystallization conditions, but the methyl group is always rejected to the lamellar interface, being smooth and flat. M39 molecules, on the other hand, take staggered alignment between the neighboring extended chains with the relative translation of a half main chain length to achieve unique packing of the central methyl branch in cooperation with end methyl groups, so that no flat surface is observed.

Attachment of bulky side groups such as hydrocarbons or aromatic compounds without having any specific interaction to the center of the main chain does not contribute to stabilization of the crystal structure but greatly impedes crystallization kinetics. The inhibition increases with the size of the branch. Even if the main chain carbon number is small, the main chain might take a once-folded conformation so that the bulky side groups may be rejected on the lamellar interface, or the sample cannot crystallize any more but might become a glass-forming material in an extreme case at low temperature. Thus it seems meaningful to perform a systematic study on branching effects on solid structures of alkanes that contain branches with various lengths or different chemical structures in the center of an otherwise linear chain taking the extended conformation in the crystalline state.

In this study, we synthesized four branched *n*-alkane samples C35−C1, C35−C4, C35−C6, and C35−C4Ph with the same carbon number of the main chain, $n = 35$, to which the methyl,

* To whom correspondence should be addressed. Tel:+8192-583-8820, E-mail: yamamoto@mm.kyushu-u.ac.jp.

† Present address: Sakata Inx, 4-1-12 Kitagawara, Itami 664-8507, Japan.

10.1021/jp044119w CCC: $30.25
Published on Web 05/11/2005

SCHEME 1

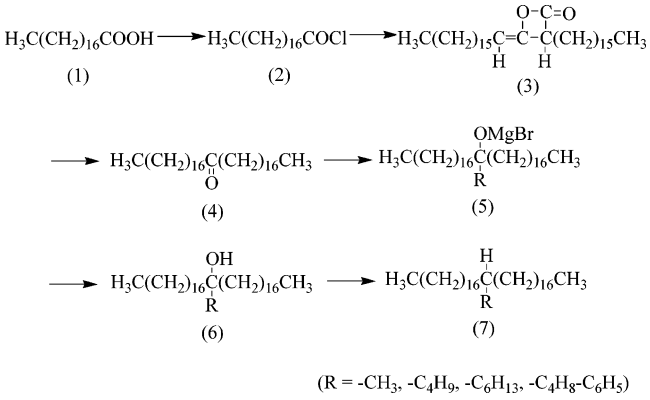

butyl, hexyl, and butyl phenyl groups were respectively attached at the middle, and also the corresponding linear homologue of C35. The first three branched alkane samples were used to study the branch length effect, and the last one was chosen to give more disturbances to crystallization kinetics and resulting equilibrium structure. We studied their crystalline structures from DSC, IR, and Raman spectroscopy, X-ray diffraction measurement, and computer simulation. We find that main chains of branched alkane molecules are not folded, irrespective of length and chemical structure of branches, but are extended to take the planar zigzag form in the solid state. The branches of C35−C4 and C35−C6 are also aligned inside the crystal in the extended form. Data analyses on solution-grown crystallized samples reveal that, with increasing the branch length, their crystal structures transform from polymorphic forms of the orthorhombic form ($P2_12_12_1$) and the triclinic form ($P\bar{1}$) for C35−C1 and C35−C4 to the unique triclinic form for C35−C6 and C35−C4Ph so as to minimize extra surface energy invoked by introduction of long branches.

Experimental Section

Materials. A series of branched alkane samples with the main chain carbon number of 35 and with a branch at the middle were synthesized through keten dimerization and Grignard reaction using the corresponding carbonic acid chlorides free from other homologues. Branches attached are methyl, butyl, hexyl, and butyl phenyl groups, and the samples are denoted C35−C1, C35−C4, C35−C6, and C35−C4Ph, respectively. The corresponding linear *n*-alkane C35 was also synthesized for comparison.

As shown in Scheme 1, carboxylic acid chloride (**2**) synthesized from corresponding carboxylic acid (**1**) (Sigma Co.; purity minimum 99.0%) and thionyl chloride in argon atmosphere was further reacted in ether solution with tertiary amine to obtain alkyl ketene dimer (**3**). Symmetrical ketone (**4**) with a carbonyl group at the middle of the main chain was easily obtained from hydrolysis of (**3**). C35 was synthesized by reducing the corresponding ketone (**4**) using the Wolff−Kishner method.[25]

Tertiary alcohol (**6**) was synthesized through the product (**5**) of the meso compound from symmetrical ketone (**4**). Powders of symmetrical ketone (**4**) were poured into an ether solution of a Grignard reagent (R−MgBr) and reacted in a nitrogen atmosphere at room temperature for 72 h. Hydrolysis of the solution of (**5**) by dropwise addition of aqueous solution saturated with ammonium chloride yielded the product (**6**).[26] After evaporation of solvent the product was confirmed as a tertiary alcohol (**6**) from IR measurement and gas chromatography. The tertiary alcohol (**6**) was reduced in dichloromethane containing trimethylsilane and trifluoroacetic acid as reducing agents for 72 h at room temperature. In an earlier synthetic method of C39−C1 denoted M39 in the report,[23] a double bond was occasionally introduced as a result of a side reaction in the main or the side chain through an intermediate stage of carbocation generation, which necessitated the additional hydrogenation reaction for conversion of the double bond into the single bond. This side reaction was completely suppressed by the use of the new reducing agent. Products obtained were finally purified by elution and recrystallization through a silica column using hexane as solvent.

Referring to an earlier study,[23] we chose toluene and butanone for solution grown (SG) crystallization of pure C35 and C35−C1, respectively. Butyl alcohol was used for SG crystallization of other branched alkanes, because crystallization is found to take place at around room temperature. It is to be noted that we could not obtain a crystallized branched alkane sample from 3% toluene solution at a temperature as low as 250 K. Homologous purities of C35, C35−C1, −C4, −C6, and −C4Ph were determined by a capillary gas chromatograph (GC-14A, Shimazu) as 99.9%, 99.3%, 98.6%, 98.4%, and 98.0%, respectively. Their densities were measured with a Gay-Lussac pycnometer as 0.836, 0.913, 0.919, 0.935, and 0.943 g cm^{-3}, respectively. Here the samples were not sufficiently compressed to avoid possible destruction of their crystalline structures by high-pressure applied.[23]

Methods. DSC measurements were performed using a calorimeter (DSC-8240B with a TAS-100 controller, Rigaku) from 293 to 363 K for all samples. The standard heating rate of 1.0 K min^{-1} was employed under dry nitrogen atmosphere for a sample mass of about 1.0 mg. The heating rate dependence was examined for a few samples of branched alkanes chosen randomly and was found negligible. Temperature calibration was performed using indium (In) and also shorter *n*-alkanes with known equilibrium melting temperatures. The heat of transition or fusion was calibrated using In and gallium.

IR spectra were obtained at room temperature using a FT-IR spectrometer (FTS-6000, Bio-Rad) with 64 scans at the highest resolution of 2 cm^{-1}. The X-ray diffraction measurements were performed for C35, C35−C1, −C4, −C6, and −C4Ph with a diffractometer using Ni-filtered Cu Kα radiation (Rigaku, Geigerflex 2027) at room temperature. Raman spectra were obtained for all samples with an NR-1800 Raman spectrometer (Japan Spectroscopic Co.) at room temperature. A beam line with 514.5 nm of wavelength from an argon ion laser was used as an excitation light source. To find the energetically most stable crystal structure, a commercial software Polymorph Predictor, a module of Cerius^2 (version 4.0, Accelrys Inc.), was used. The potential functions used were of COMPASS force field. The unit cell parameters of the crystal structural models obtained were slightly modified so that they may give better reproduction of X-ray diffraction data taken at room-temperature, keeping essential features of the structure unchanged. These modified structures were minimized again under the assumption of rigid body molecules.

Results and Discussion

Thermal Behaviors. Figure 1 shows DSC curves of the linear alkane C35 and four branched alkanes C35−C1, −C4, −C6, and −C4Ph. The curve of C35 unambiguously exhibits the B, C, and H solid−solid-phase transitions at 332, 339, and 345 K, respectively, and a sharp melting peak at 347.5 K. The very small peak of the A′ phase transition reported earlier[27] was not

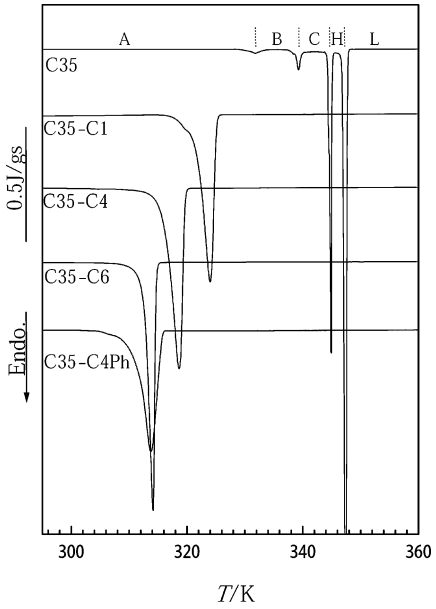

Figure 1. DCS curves for the linear alkane C35, and branched alkanes C35−C1, −C4, −C6, and −C4Ph as indicated.

TABLE 1: Enthalpy, Entropy, and Melting Temperature of C35, C35−C1, C35−C4, C35−C6, and C35−C4Ph

sample	ΔH/kJ mol^{-1}	ΔS/kJ mol^{-1}K^{-1}	T_m/K
C35	135	0.39	347.5
C35−C1	99	0.30	325.2
C35−C4	104	0.32	318.5
C35−C6	107	0.34	314.3
C35−C4Ph	94	0.30	314.1

observed in this measurement. On the other hand, there is no solid−solid phase transition peak for branched alkanes, and their melting peaks observed are broad as compared with the peak of C35, and their melting temperatures T_m are 325.2, 318.5, 314.3, and 314.1 K, respectively. The melting temperature of C35−C1 is the highest of branched alkanes tested, nonetheless being lower by more than 20 K in comparison with T_m of C35. T_m is likely to decrease with increasing the branch length. Lowering of T_m and broadening of the endothermic peak are related to the fact that we were unsuccessful in preparation of the single crystal with a mm size for branched alkanes, which are forced to take a more or less disordered crystal due to a difficulty of branched alkane molecules in achieving close parallel chain packing.

We calculated enthalpy ΔH and entropy ΔS associated with melting of C35 and branched alkanes from area of respective endothermic peaks on DSC curves. ΔH and ΔS of branched alkanes listed in Table 1 are all lower than those of C35. In comparing ΔH and ΔS data of four branched alkane samples, we became aware of that larger ΔH and ΔS values observed for C35−C6 and −C4, as well as their relatively sharp melting peaks shown in Figure 1, might be originated from crystallization of branches, which partly contributes for stabilization of the whole crystal. This conjecture shall be discussed in connection with the Raman data later. The smallest ΔH and ΔS values observed for C35−C4Ph strongly suggest that the bulky phenyl ring distorts the parallel chain packing of the main chains considerably.

IR Absorption. We performed IR absorption measurements on a powder-like crystal for all samples, which were carefully sandwiched between two KBr plates to minimize possible disturbances or alteration of crystalline structures of the fragile samples by applied pressure. Figure 2 gives IR spectra

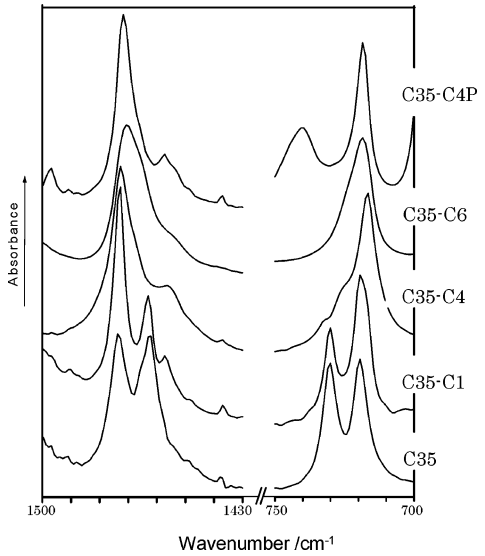

Figure 2. IR spectra for C35 and branched alkanes C35−C1, −C4, −C6, and −C4Ph in the two wavenumber regions of 700−750 cm^{-1} and 1430−1500 cm^{-1}.

of C35 and four branched alkane samples in relatively narrow wavenumber regions of 700−750 cm^{-1} and 1430−1500 cm^{-1} at room temperature. It is to be noted that completely different IR spectra were indeed obtained for the C35−C1 sample prepared with such a conventional method that the samples are mixed well with KBr powder and then pressed to make the disk.

For an orthorhombic type of subcell structure, the IR absorption bands at 720 cm^{-1}, corresponding to the CH_2 rocking mode, and at 1473 cm^{-1}, corresponding to the CH_2 scissors mode, are known to be split into two components due to intermolecular interaction, whereas there occurs no splitting for a triclinic or a monoclinic type. The well split IR bands are seen in the spectrum of C35 as expected for the orthorhombic type of crystal in the A phase. Splitting is also clearly observed in the spectrum of C35−C1 at the same wavenumbers as C35, although there are considerable differences in intensities of respective components for both of the modes originated from disordering of the crystalline structure. These results suggest that C35−C1 takes an orthorhombic type of subcell structure mainly. On the other hand, C35−C6 and C35−C4Ph give single absorption bands at 730 cm^{-1} and 1473 cm^{-1}, characteristic of a monoclinic or triclinic type. C35−C4 also gives strong absorption bands at the same wavenumbers accompanied by shoulders, which implies the presence of a small amount of crystal having the orthorhombic type of subcell structure. For C35−C4Ph, the peaks at 740 and 1450 cm^{-1} are assigned to the out-of-plane CH deformation mode and to the C=C deformation mode in the phenyl ring, respectively.

X-ray Diffraction Measurement. Figure 3 shows X-ray diffraction profiles of C35 and four branched alkanes measured at room temperature in a range of diffraction angles 2θ from 1.5° to 45.0°. Linear alkane C35 gives a sequence of sharp diffraction peaks over a wide diffraction angle range corresponding to (00l) reflections of the long spacing, with even number of l along the main chain c axis. Linear alkane C35 also has peaks at $2\theta = 21.5°$ and $2\theta = 23.8°$ from the (110) and (200) planes, characteristic of linear alkanes with odd carbon number at room temperature, i.e., of the A structure.[3] For C35−C1, on the other hand, only a small number of broad diffraction peaks are seen in the low diffraction angle region, whereas three strong peaks in the 2θ range from 19° to 23°

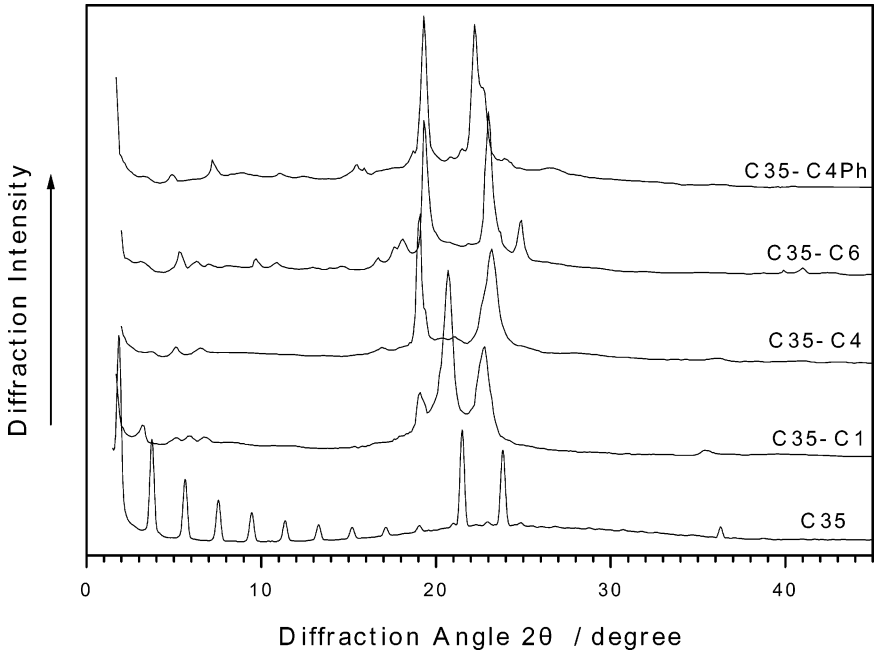

Figure 3. X-ray diffraction profiles for the linear alkane C35, and branched alkanes C35−C1, −C4, −C6, and −C4Ph.

and an additional peak at 35.5° are observed. The whole diffraction profile is, in appearance, quite similar to that of M39, which has been found to be present in polymorphic forms: one the orthorhombic form and another the triclinic form. Thus it seems reasonable to suppose that C35−C1 is also a polymorph as M39. Determination of lattice parameters corresponding to respective crystal structures shall be done after description of the Raman scattering data and results of computer simulation.

Neither of the three other branched alkane samples gives sharp peaks in the low 2θ region. This is not an unexpected result for powder-like crystals, whereas broadness of peaks may be due to the small coherent domain size proved by X-ray diffraction measurement or due to superposition of two or even three peaks. With increasing the length or the size of the branch, however, diffraction profiles appear to become more complex with a considerable number of weak peaks in the 2θ range from 10° to 19° accompanied by a sharp increase in an intensity of a peak at around $2\theta = 19°$. The latter is consistent with a triclinic type of crystal structure disclosed by the IR spectra. If conformation of single branched alkane molecules in the crystalline state is unambiguously determined from Raman scattering measurement, then we may be allowed to determine the crystal structure of C35−C6 and −C4Ph using the conventional method for X-ray diffraction data analysis unequivocally. It appears a little bit difficult to determine the crystal structure of C35−C4, because of a small number of diffraction peaks.

Raman Scattering. Conformation of the main chain or the chain length in the crystalline state can be unambiguously determined from Raman scattering measurements using vibration modes of the longitudinal acoustic mode (LAM), if the chain is depicted as an isolated continuous elastic rod. The *j*th LAM frequency of the vibration, ν_j, is given by

$$\nu_j = (j/2cL)(E_c/\rho)^{1/2} \quad (1)$$

where c is the speed of light in the medium, E_c is Young's modulus of the chain in the solid state, ρ is the density, and j is the vibration order (only odd numbers are Raman active).

Figure 4 shows results of Raman scattering measurements on C35 and all branched alkane samples at room temperature. Four peaks are clearly observed for C35 at 70.7, 193.6, 313.4, and 411.1 cm^{-1}, corresponding to the LAM modes with $j = 1$, 3, 5, and 7, respectively. The broad peak observed at 100 cm^{-1} is due to a Raman active lattice mode of rotational vibration around the main chain axis belonging to the B_{3g} symmetry species.[28] Strobl and Eckel pointed out, from Raman scattering experiments on linear alkanes C_nH_{2n+2} with $33 \le n \le 94$, that weak interlamellar forces result in an upward shift of ν_j given by eq 1, and proposed the following empirical equation:[29]

$$\nu_j = 2236j/(n - 1.6) + 2.2/j \quad (2)$$

Table 2 shows the comparison of LAM frequencies measured with those calculated from eqs 1 and 2. Equation 2 gives $\nu_1 =$ 69.15 cm^{-1} for $n = 35$, which is in excellent agreement with the experimental value of $\nu_1 = 70.7$ cm^{-1}, and also gives $\nu_3 =$ 201.6 cm^{-1}, $\nu_5 = 335.2$ cm^{-1}, and $\nu_7 = 468.9$ cm^{-1}, being slightly higher than the values measured.

Four peaks are also observed for all branched alkane samples. These are in excellent agreement with corresponding ν_j values of C35, as shown by dotted vertical lines in Figure 4. Because C35 molecules are known to take the extended chain conformation, forming the orthorhombic type of crystal, we conclude that main chains of branched alkane molecules are not folded, irrespective of length and chemical structure of branches, but are extended so as to take the planar zigzag form in the solid state. The LAM frequencies primarily depend on the main chain length as well as the intramolecular interaction forces, and their small frequency shifts are brought by the intermolecular forces.[30] Close agreement of ν_j values between C35 and all branched alkanes indicates that intermolecular interactions responsible for symmetrical longitudinal backbone vibration modes are almost the same for those samples, even though the branch groups attached to the center of the main chain of all branched alkanes must be located inside the lamellae and are expected to perturb the chain packing to some extent.

In addition to the LAM mode of the main chain, another peak is observed at 554.2 cm^{-1} for C35−C4 and at 388.9 cm^{-1} for

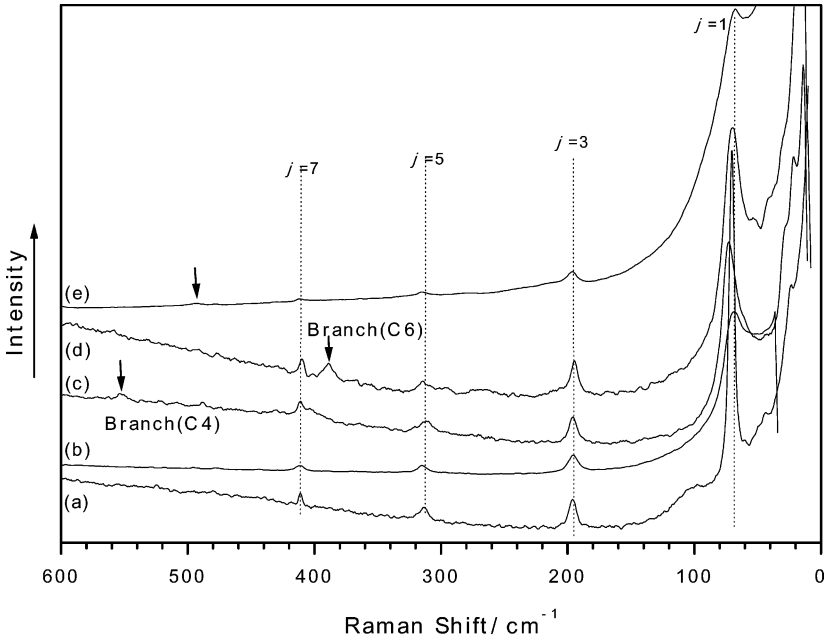

Figure 4. Raman spectra from longitudinal acoustic modes (LAM) for the linear alkane (a) C35, and branched alkanes (b) C35−C1, (c) C35−C4, (d) C35−C6, and (e) C35−C4Ph.

TABLE 2: Comparison of the Vibration Frequencies of the Longitudinal Acoustic Mode Measured with Those Calculated from Equations 1 and 2

			calculation		measurement			
	n	*j*	theoretical equation[a]	empirical equation[b]	C35	C35−C4	C35−C6	C35−C4Ph
main chain	35	1	68.57	69.15	70.7	72.6	69.4	67.5
		3	205.71	201.57	193.6	195.6	195.0	196.3
		5	342.86	335.17	313.4	312.1	314.1	315.3
		7	480.00	468.94	411.1	411.1	409.8	414.1
branched chain	4	1	600.00	933.87		554.2		
	6	1	400.00	510.38			388.9	

[a] $\nu_j = (j/2cL)(E_c/\rho)^{1/2} \approx 2400j/n$. [b] $\nu_j = 2236j/(n - 1.6)+2.2/j$ ($j = 1, 3, 5...$). Here, c: speed of light, E_c: Young's modulus, ρ: density, n: carbon number; j: vibration order (only odd numbers are Raman active).

C35−C6, respectively, which are in agreement with the theoretical values of $\nu_1 = 600$ cm^{-1} and $\nu_1 = 400$ cm^{-1} given by eq 1 as the LAM mode of C4 and C6 branches, respectively. In the preceding 'Thermal Behaviors' section, we suggested that short alkane chains of C4 and C6 may be regularly aligned on the crystalline lattice. The Raman results unambiguously indicate that both the main chain and the branch of C35−C4 and −C6 take the extended chain conformation and contribute to crystal formation. A very small peak is also seen in the Raman spectrum of C35−C4Ph at 493.2 cm^{-1}, being intermediate between those for C35−C4 and −C6. This might correspond to the LAM mode of the C4Ph branch. However, such the assignment seems premature, since the melting peak in Figure 1 is rather broadened by introduction of the C4Ph group and also the Raman band corresponding to the bending mode of the phenyl ring or the twisting mode of the carbon-phenyl bond may appear in this frequency region.

Computer Simulation. Computer simulation played an important role for determination of crystal structures of M39 taking polymorphic forms, since it was formidably difficult to evaluate lattice parameters accurately from a limited small number of X-ray diffraction peaks. SG crystallized M39 has been found to take polymorphic forms composed of the $P2_12_12_1$ and the $P\bar{1}$ space groups, and the peaks are successfully indexed. Since the diffraction profile of C35−C1 is similar to that of SG-M39, we performed computer simulations assuming that C35−C1 also takes the same polymorphic form as M39. Two space groups of $P2_12_12_1$ and $P\bar{1}$ are indeed found to reproduce X-ray diffraction patterns shown in Figure 3 fairly well with indices given in Table 3. The predicted molecular model belonging to the $P2_12_12_1$ space group gives unit cell dimensions as $a = 1.515$ nm, $b = 0.505$ nm, $c = 4.858$ nm, and $\alpha = \beta = \gamma = 90°$, and the density 0.904 g cm^{-3} is close to the experimental value of 0.913 g cm^{-3} obtained for C35−C1. The unit cell contains four C35−C1 molecules as found for C35 taking

TABLE 3: Comparison of Diffraction Angle 2θ Measured with Those Calculated for C35−C1

experimental		crystalline lattice calculated			
		$P\bar{1}$[a]		$P2_12_12_1$[b]	
2θ/degree	*d*/nm	2θ/degree	(*hkl*)	2θ/degree	(*hkl*)
3.2 (w)	2.75			3.6	(002)
5.1 (vw)	1.72				
5.9 (vw)	1.49			5.9	(101)
7.0 (vw)	1.26			7.2	(004)
19.1 (vs)	0.46	19.1	(200)		
20.7 (vs)	0.43	20.7	(010)	20.7	(210)
22.8 (vs)	0.39	22.8	(210)	22.8	(400)
35.5 (vw)	0.25			35.1	(020)

[a] $P\bar{1}$: $a = 1.069$ nm, $b = 0.480$ nm, $c = 4.693$ nm, $\alpha = 72.6°$, $\beta = 68.0°$, $\gamma = 65.0°$, density = 0.845 g cm^{-3}. [b] $P2_12_12_1$: $a = 1.515$ nm, $b = 0.505$ nm, $c = 4.858$ nm, $\alpha = \beta = \gamma = 90°$, density = 0.904 g cm^{-3}.

TABLE 4: Comparison of Diffraction Angle 2θ Measured with Those Calculated for C35−C6

experimental		crystalline lattice calculated $P\bar{1}$[a]	
2θ/degree	*d*/nm	2θ/degree	(*hkl*)
3.1 (w)	28.4	3.2	(002)
5.3 (m)	16.5	5.5	(101)
6.4 (w)	13.9	6.4	(004)
			(10$\bar{1}$)
9.6 (w)	9.1	9.6	(006)
10.9 (w)	8.1	11.0	(201)
		11.1	(202)
16.7 (w)	5.3	16.8	(301)
		17.1	(300)
17.6 (w)	5.0	17.6	(30$\bar{1}$)
18.1 (m)	4.9	18.3	(302)
19.3 (vs)	4.6	19.3	(010)
21.9 (w)	4.1	21.5	(110)
23.0 (vs)	3.9	23.0	(400)
24.9 (s)	3.6	24.9	(210)
39.9 (w)	2.3	39.8	(024)
40.9 (w)	2.2	41.1	(120)

[a] $P\bar{1}$: $a = 1.656$ nm, $b = 0.474$ nm, $c = 5.726$ nm, $\alpha = 90.0°$, $\beta = 75.0°$, $\gamma = 103.9°$, density $= 0.912$ g cm^{-3}.

the double layer structure, but the lattice parameters *a*, *b*, and *c* are different from $a = 0.749$ nm, $b = 0.496$ nm, and $c = 9.330$ nm of C35. The closest packing of end methyl groups at the interface in the C35 crystal gives rise to the relative translation of linear alkane molecules along the *a* axis in the upper and the lower layers; thus *c* becomes a double of the main chain length. As found for M39,[23] four adjacent extended chains surrounding one C35−C1 molecule in the C35−C1 crystal relatively translate by a half of the main chain length along the *c* axis to accommodate the central methyl group under cooperation of end methyl groups, which affects directions of chain planes of the next nearest neighbor chains, resulting in the unit cell with the large *a*. Nevertheless, introduction of the central methyl group very slightly loosens the local chain packing to a similar extent along all three axial directions. The lattice parameters estimated for the $P\bar{1}$ triclinic type of crystal are $a = 1.069$ nm, $b = 0.480$ nm, $c = 4.693$ nm, $\alpha = 72.6°$, $\beta = 68.0°$, and $\gamma = 65.0°$, and the density is 0.845 g cm^{-3}. The unit cell contains two M39 molecules due to staggered alignment between adjacent chains with the relative translation of a half main chain length and chain planes of all molecules oriented to the same direction. The $P\bar{1}$ triclinic structure proposed is different from those of even alkanes from $C_{10}H_{22}$ to $C_{26}H_{54}$ in which end-methyl groups are disposed on the flat interface so as to achieve dense packing.[31−36] It is to be noted that, if unit cell structures given by the two models are realized in the C35−C1 crystal, intensities from (00*l*) reflections should be considerably lowered in comparison with those of C35. The orthorhombic model successfully predicts four peaks of C35−C1 at $2\theta = 20.7°$, 22.8°, and 35.1° and also three broad peaks at low angles as reflections from (002) and (004), and (101) planes. However, this model cannot give the strong peak at $2\theta = 19.1°$, which leads to the fact that C35−C1 is present in polymorphic forms, one being the orthorhombic form and another the triclinic form, with approximate lattice parameters obtained. Three strong peaks of C35−C1 at $2\theta = 19.1°$, 20.7°, and 22.8° appear to be represented by the triclinic model. The model gives (002) and (003) reflections at $2\theta = 4.12°$, and 6.18°, but no peak is seen at those angles. Instead, very weak and broad peaks are seen at $2\theta = 3.2°$ and 7.0°, which are in fair agreement with (002) and (004) reflections of the orthorhombic model, whose main peaks are located at $2\theta = 20.7°$ and 22.8°. These molecular models were illustrated in Figures 7 and 8 in the earlier report,[23] which

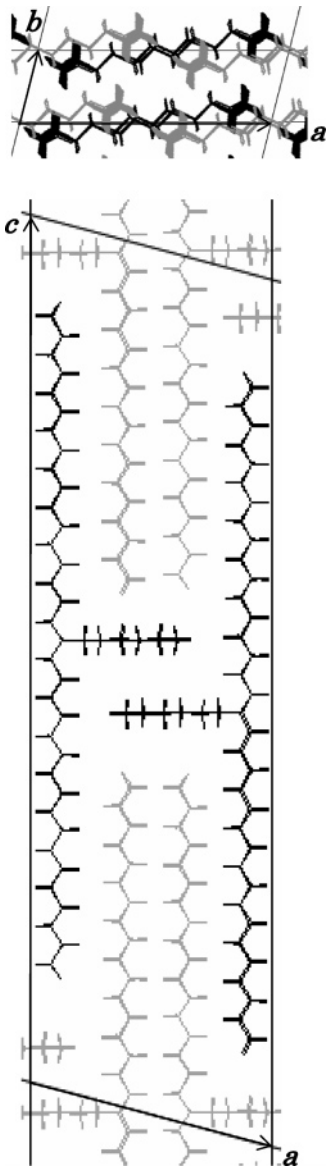

Figure 5. Molecular model of C35−C6 for the space group $P\bar{1}$: $a = 1.656$ nm, $b = 0.474$ nm, $c = 5.726$ nm, $\alpha = 90°$, $\beta = 75°$, and $\gamma = 103.9°$.

gives a characteristic feature that there exists no smooth flat interface where methyl groups are disclosed. Instead, all methyl groups are located inside the crystal, which gives rise to staggered alignment between neighboring extended chains. Thus it does not seem unreasonable to suppose that chain stacking along the main chain axis is quite difficult.

Computer simulation for C35−C4, −C6, and −C4Ph was made for five space groups, $P2_1$, $P2_12_12_1$, $P2_1/c$, $C2/c$, and $P\bar{1}$, among which $P\bar{1}$ was found to be the most stable. It gave large unit cell dimensions so as to accommodate extended long branches inside the crystals formed by extended main chains. None of the molecular models predicted, however, failed to reproduce the X-ray diffraction patterns very well, even after slight modification of lattice parameters.

Crystal Structures of C35−C6 and C35−C4Ph. Since a considerable number of peaks are observed on the X-ray diffraction curve of C35−C6, we attempted to determine its crystal structure based on the experimental results that the crystal belongs to the $P\bar{1}$ space group with extended chain conformation for the both main chain and the branch. It turned out that only the unit cell composed of four molecules, as predicted by

TABLE 5: Comparison of Diffraction Angle 2θ Measured with Those Calculated for C35−C4Ph

experimental		crystalline lattice calculated $P\bar{1}$ [a]	
2θ/degree	d/nm	2θ/degree	(hkl)
3.5 (w)	25.3	3.5	(002)
4.9 (w)	15.2	5.2	(101)
7.3 (m)	12.1	7.0	(004)
11.1 (w)	8.0	11.0	(200)
15.5 (w)	5.7	15.7	(303)
15.9 (w)	5.6	15.8	(30$\bar{2}$)
18.8 (w)	4.7	19.0	(30$\bar{3}$)
19.3 (vs)	4.6	19.3	(010)
20.8 (w)	4.3	20.9	(404)
21.5 (w)	4.1	21.6	(401)
22.2 (vs)	4.0	22.2	(400)
22.8 (s)	3.9	22.8	(21$\bar{0}$)
23.6 (w)	3.8	23.6	(40$\bar{2}$)
23.9 (w)	3.7		
24.3 (w)	3.7	24.4	(40$\bar{3}$)
26.5 (w)	3.4	26.2	(31$\bar{0}$)
		26.6	(311)

[a] $P\bar{1}$: $a = 1.732$ nm, $b = 0.508$ nm, $c = 5.909$ nm, $\alpha = 115.0°$, $\beta = 68.0°$, $\gamma = 101.4°$, density $= 0.953$ g cm^{-3}.

TABLE 6: Comparison of Diffraction Angle 2θ Measured with Those Calculated for C35−C4

		crystalline lattice calculated			
experimental		$P\bar{1}$ [a]		$P2_12_12_1$ [b]	
2θ/degree	d/nm	2θ/degree	(hkl)	2θ/degree	(hkl)
3.7 (vw)	23.6	3.7	(002)	3.5	(002)
5.1 (w)	17.3	5.2	(10$\bar{1}$)	5.7	(100)
6.6 (w)	13.5	6.6	(10$\bar{1}$)	7.0	(004)
17.0 (w)	5.2	16.9	(300)		
19.0 (vs)	4.7	19.0	(010)		
20.4 (w)	4.4	20.4	(1$\bar{1}$0)		
21.0 (w)	4.2	21.1	(2$\bar{1}$0)	21.0	(210)
23.2 (vs)	3.8	23.2	(210)	23.2	(400)
		23.6	(400)		
35.4 (vw)	2.5			35.4	(020)

[a] $P\bar{1}$: $a = 1.707$ nm, $b = 0.491$ nm, $c = 5.368$ nm, $\alpha = 72.6°$, $\beta = 68.0°$, $\gamma = 89.1°$, density $= 0.921$ g cm^{-3}. [b] $P2_12_12_1$: $a = 1.534$ nm, $b = 0.507$ nm, $c = 4.977$ nm, $\alpha = \beta = \gamma = 90°$, density $= 0.943$ g cm^{-3}.

computer simulation, can reproduce the observed X-ray diffractogram. Table 4 compares diffraction angles 2θ measured with those calculated from the molecular model whose unit cell dimensions are $a = 1.656$ nm, $b = 0.474$ nm, $c = 5.726$ nm, $\alpha = 90°$, $\beta = 75°$, and $\gamma = 103.9°$. The density 0.912 g cm^{-3} calculated is close to the measured value of 0.935 g cm^{-3}. Excellent agreement allows us to conclude that C35−C6 forms a triclinic type of crystal. As is shown in Figure 5, the unit cell is expanded toward the *a* and the *c* axes in order to accommodate the long branch chain along the *a* axis as well as to help vertical alignment of two adjacent branches along the *c* axis in the solid state.

Since the branch length of C4−Ph is comparable to that of C6 in their extended forms, C35−C4Ph is likely to take a triclinic type of crystal with sizes of the unit cell similar to those of C35−C6. Making use of a considerable number of peaks on the X-ray diffraction curve of the sample, we could successfully index the peaks excluding the weak peak at $2\theta = 23.9°$, as given in Table 5. The unit cell dimensions are $a = 1.732$ nm, $b = 0.508$ nm, $c = 5.909$ nm, $\alpha = 115°$, $\beta = 68°$, and $\gamma = 101.4°$. The size is a little bit larger than those of C35−C6 probably as being due to the bulky phenyl group. The density 0.952 g cm^{-3} is once again close to the measured value of 0.943 g cm^{-3}. It is uncertain if phenyl rings are regularly aligned in the solid state. Introduction of the bulky phenyl group does not seem to affect formation of the same crystalline structure as C35−C6, but results in a perturbed structure as revealed by the broad melting peak from DSC.

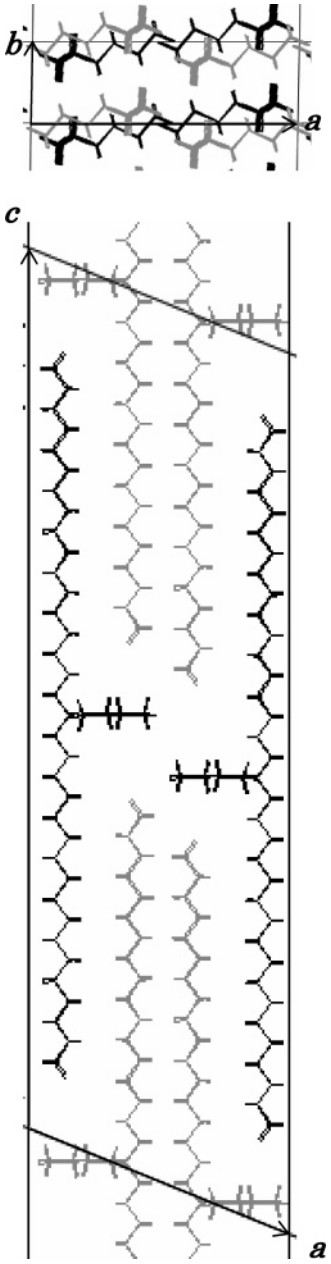

Figure 6. Molecular model of C35−C4 for the space group $P\bar{1}$: $a = 1.707$ nm, $b = 0.491$ nm, $c = 5.368$ nm, $\alpha = 72.6°$, $\beta = 68.0°$, and $\gamma = 89.1°$.

Crystal Structure of C35−C4. As described in an earlier section, a small number of X-ray diffraction peaks of this sample shown in Figure 3 may not provide information sufficient for determination of the crystal structure. Now, however, we know that the unit cell of C35−C1 crystal belonging to the $P2_12_12_1$ space group is composed of four molecules and also unit cells of C35−C6 and −C4Ph belonging to the $P\bar{1}$ space group are composed of four molecules irrespective of their different branch structures. This leads us to supposition that C35−C4 also contains four molecules in the unit cell and is present most generally in polymorphic forms of the $P\bar{1}$ and the $P2_12_12_1$ crystals as suggested by IR data. Table 6 gives results of analysis of the X-ray diffraction data. It seems that the $P\bar{1}$ crystal is dominantly formed in C35−C4, judging from the presence of

the very strong peaks at $2\theta = 19.0°$ and 23.2° as well as good reproducibility of the peaks in the low diffraction angle range, but the weak peaks at $2\theta = 21.0°$ and 35.4° are more reasonably explained if a small fraction of the $P2_12_12_1$ crystal is present in the sample. Figure 6 illustrates the unit cell structure of C35−C4 belonging to the $P\bar{1}$ space group predicted, which is close to that of C35−C6 despite the shorter branch length. The model is consistent with the Raman data that all C4 branched chains are regularly aligned in the extended form and contribute for stabilization of the crystal to some extent. Computer simulation was once again performed to examine conformations of the main and the branch chains using the unit cell dimensions given in Table 6. Results show that two of mains chains and the C4 branch take extended conformation, whereas remaining two chains are found to be slightly bent. The extra bending energy might partially explain why C35−C4 is present in polymorphic forms.

Concluding Remarks

In this study, we examined effects of length and chemical structure of a branch attached to the middle of *n*-alkane chain with the carbon number $n = 35$ on crystal structures using four branched alkane samples of high purity. Raman data showed that main chains of branched alkane molecules are not folded, irrespective of length and chemical structure of branches examined, but are extended to take the planar zigzag form in the solid state and also that butyl and hexyl branches are aligned in the extended form. Data analyses on solution-grown crystallized samples revealed that introduction of the methyl group as the branch most severely perturbs the crystal structure, yielding polymorphic forms of the orthorhombic one ($P2_12_12_1$) as the major component and the triclinic one ($P\bar{1}$), whereas the rather stable single triclinic type of crystal is formed for the sample with the hexyl branch, which is regularly aligned in the crystalline lattice so as to minimize extra surface energy invoked by introduction of long branches. The sample with the butyl branch is polymorph with the $P\bar{1}$ crystal as the major component, and the bulky butyl phenyl branch gives rise to a distorted $P\bar{1}$ crystal with a similar size of the unit cell dimensions as the sample with the hexyl branch. A characteristic feature is that there exists no smooth flat interface where branch groups are disclosed. Instead, all branch groups are located inside the crystal due to adequate relative translation of molecules by a half of the main chain length along the *c* axis to accommodate the central branch group under cooperation of end methyl groups. Then a question arises as to what branch length this kind of unique crystal structures persists. We recently synthesized a symmetrical branched alkane of a three-arm star type with the arm carbon number of 17. Preliminary experiments show that chain folding takes place at the center and the flat surface is recovered between lamellae with thickness corresponding to the arm length. Details shall be reported in a forthcoming paper.

References and Notes

(1) Smith, A. E. *J. Chem. Phys.* **1953**, *21*, 2229.
(2) Shearer, H. M. M.; Vand, V. *Acta Crystallogr.* **1956**, *9*, 379.
(3) Pieszek, W.; Strobl, G. R.; Makahn, K. *Acta Crystallogr.* **1974**, *B30*, 1278.
(4) Dawson, I. M. *Proc. R. Soc. (London)* **1952**, *A214*, 72.
(5) Takamizawa, K.; Urabe, Y.; Fujimoto, J.; Ogata, H.; Ogawa. Y. *Thermochim. Acta* **1995**, *267*, 297.
(6) Takamizawa, K.; Ogawa, Y.; Oyama, T. *Polym. J.* **1982**, *14*, 441.
(7) Urabe, Y.; Yanaka, S.; Fujinaga, M.; Yamamoto, H.; Takamizawa, K. *Polym. J.* **1997**, *29*, 534.
(8) Saville, W. B.; Shearer, G. *J. Chem. Soc*. **1925**, *127*, 591.
(9) Muller, A.; Saville, W. B. *J. Chem. Soc.* **1925**, *127*, 599.
(10) Piper, S. H.; Chibnall, A. C.; Hopkins, S. J.; Pollard, A. J.; Smith, A. B.; Williams, B. F. *Biochem. J.* **1931**, *25*, 2072.
(11) Oldham, J. W. H.; Ubbelohde, A. R. *Trans. Faraday Soc.* **1939**, *35*, 328.
(12) Takamizawa, K.; Nakasone, K.; Urabe, Y.; Sonoda, T. *Eng. Sci. Rep. Kyushu U.* **1990**, *12*, 291 (in Japanese).
(13) Takamizawa, K.; Nakasone, K.; Urabe, Y. *Colloid Polym. Sci*. **1994**, *272*, 293.
(14) Nakasone, K.; Urabe, Y.; Takamizawa, K. *Thermochim. Acta* **1996**, *286*, 161.
(15) Nakasone, K.; Shiokawa, K.; Urabe, Y.; Nemoto, N. *J. Phys. Chem. B* **2000**, *104*, 7483.
(16) Nakasone, K.; Nemoto, N., submitted to *Bull. Chem. Soc.*, Japan.
(17) Kimoto, H.; Yamamoto, H.; Urabe, Y.; Shiokawa, K.; Nemoto, N., submitted to *Bull. Chem. Soc*., Japan.
(18) Muller, A. *Proc. R. Soc. A* **1932**, *138*, 514.
(19) Bunn, C. W. *Trans. Faraday Soc.* **1939**, *35*, 482.
(20) Buroadhurst, M. G. *J. Res. Natl. Bur. Stand.* **1962**, *66A*, 241.
(21) Mandelkern, L.; Prasad, A.; Alamo, R. G.; Stack, G. M. *Macromolecules* **1990**, *23*, 3696.
(22) Takamizawa, K.; Ogawa, Y.; Oyama, T. *Polym. J.* **1982**, *14*, 441.
(23) Yamamoto, H.; Nemoto, N.; Tashiro, K. *J. Phys. Chem. B* **2004**, 108, 5827.
(24) Ungar, G.; Zeng, X. B. *Chem. Rev*. **2001**, *101*, 4157.
(25) Bidd, I.; Whiting, M. C. *J. Chem. Soc., Chem. Commun*. **1985**, *9*, 543.
(26) Wakefield, B. J. *Organomagnesium Methods in Organic Synthesis*; Academic Press: London, 1995.
(27) Urabe, Y.; Takamizawa, K. *Tech. Rep., Kyushu Univ.* **1994**, *67*, 85 (in Japanese).
(28) Kobayashi, M.; Tadokoro, H. *J. Chem. Phys.* **1977**, *66*, 1258.
(29) Strobl, G. R.; Eckel, R. *J. Polym. Sci., Polym. Phys. Ed*. **1976**, *14*, 913.
(30) Pietralla, M.; Hotz, R.; Engst, T.; Siems, R. *J. Polym. Sci., Pt. B: Polym. Phys.* **1997**, *35*, 47.
(31) Muller, A.; Lonsdale, K. *Acta Crystallogr*. **1948**, *1*, 129.
(32) Shearer, H. M. M.; Vand, V. *Acta Crystallogr*. **1948**, *1*, 129.
(33) Norman, N.; Mathisen, H. *Acta Chem. Scand*. **1972**, *26*, 3913.
(34) Boistelle, R.; Simon, B.; Pepe, G. *Acta Crystallogr*. **1976**, *B32*, 1240.
(35) Gerson, A. R.; Roberts, K. J.; Sherwood, J. N. *Acta Crystallogr*. **1991**, *B47*, 280.
(36) Nyburg, S. C.; Gerson, A. R. *Acta Crystallogr*. **1992**, *B48*, 103.